Available online at www.sciencedirect.com
SCIENCE DIRECT®
Bioorganic & Medicinal Chemistry 12 (2004) 4823–4833
Bioorganic & Medicinal Chemistry

New 3-piperonylcoumarins as inhibitors of glycosomal glyceraldehyde-3-phosphate dehydrogenase (gGAPDH) from *Trypanosoma cruzi*

Anderson Aparecido de Marchi,[a] Marcelo Santos Castilho,[b] Paulo Gustavo Barboni Nascimento,[c] Fernando Costa Archanjo,[c] Gino Del Ponte,[a] Glaucius Oliva[b] and Mônica Tallarico Pupo[a,*]

[a]*Faculdade de Ciências Farmacêuticas de Ribeirão Preto, Universidade de São Paulo, 14040903 Ribeirão Preto, SP, Brazil*
[b]*Instituto de Física de São Carlos, Universidade de São Paulo, 13560970 São Carlos, SP, Brazil*
[c]*Faculdade de Filosofia, Ciências e Letras de Ribeirão Preto, Universidade de São Paulo, 14040901 Ribeirão Preto, SP, Brazil*

Received 22 March 2004; revised 6 July 2004; accepted 7 July 2004
Available online 6 August 2004

Abstract—This article describes the synthesis and inhibitory activities of a series of new 3-piperonylcoumarins, designed as inhibitors of glycosomal glyceraldehyde-3-phosphate dehydrogenase (gGAPDH) from *Trypanosoma cruzi*. The design was based on the structures of previously identified natural products hits. The most active synthesized derivatives contain heterocyclic rings at position 6. SAR studies, performed by electronic indices methodology (EIM), clustered the molecules in different groups due to the chemical substitutions regarding the biological activity. Molecular modeling studies by docking suggested a different binding mode for the most active derivatives, when compared to natural hit chalepin. Moreover, the coumarin ring seems to act only as a spacer group.

1. Introduction

Protozoan parasites of the Trypanosomatidae family are responsible for a wide variety of ailments, amongst them sleeping sickness and the American trypanosomiasis, also known as Chagas' disease, which is endemic to 15 countries of Latin America, where 40 million people are at risk and 200,000 new cases are registered each year.[1] Owing to their toxicity and lack of efficacy, most of the currently used compounds are unsatisfactory[2] and therefore the design of novel classes of trypanocidal drugs has become urgent. In fact, the medical and economic problems caused by Chagas' disease justify its selection by the World Health Organization for the development of new or more effective treatments.[1]

One promising approach to accomplish this task is through the selective inhibition of enzymes that participate in the glycolitic pathway of the parasite (*Trypanosoma cruzi*). Glyceraldehyde-3-phosphate dehydrogenase (gGAPDH), the sixth enzyme in the glycolytic pathway, plays an essential role in the control of glycolytic flux.[3,4] As intracellular amastigotes predominantly depend on glycolisis for ATP production, the inhibition of gGAPDH would prevent *T. cruzi* from being infective.[2,5] For this reason, it has been identified as a suitable target for the development of inhibitors. Additionally, it has been observed that 95% deficiency of GAPDH in human erythrocytes does not cause any clinical symptoms.[6]

In an on-going program to screen natural products libraries in the search for new potential inhibitors of *T. cruzi* gGAPDH, a series of natural coumarins and flavonoids isolated from the Rutaceae family were identified[7,8] (Fig. 1). The best inhibitor, a coumarin derivative, chalepin, was selected as a good hit and was co-crystallized with gGAPDH.[9] Based on the information gathered from the crystallographic structure, a computer-aided molecular design approach was undertaken, in order to better characterize the binding site of gGAPDH and thus understand the essential features for coumarin binding in the *T. cruzi* gGAPDH active site.[10] The

Keywords: 3-Piperonylcoumarins; Glycosomal glyceraldehyde-3-phosphate dehydrogenase; *Trypanosoma cruzi*; Molecular modeling.
* Corresponding author. Tel.: +55-16-6024431; fax: +55-16-6331941; e-mail: mtpupo@fcfrp.usp.br

0968-0896/$ - see front matter © 2004 Elsevier Ltd. All rights reserved.
doi:10.1016/j.bmc.2004.07.018

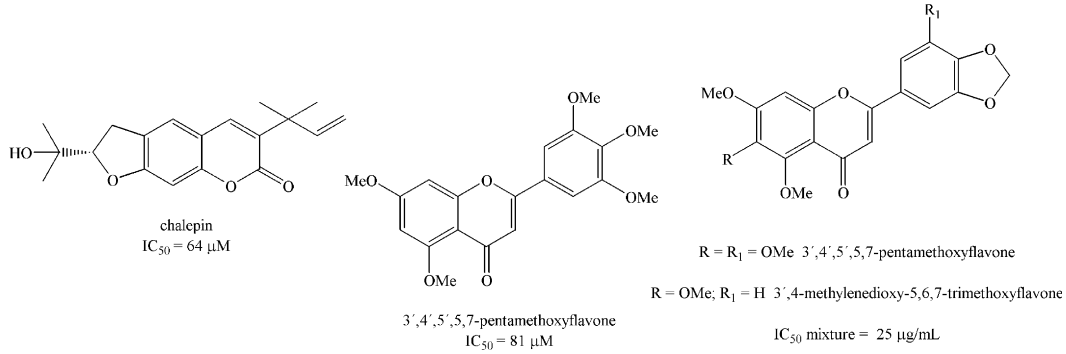

Figure 1. Natural products hits and their gGAPDH inhibitory activities.[7,8]

analysis of the 3D QSAR model obtained in this study suggests that the crucial features for binding are the lipophilic character of the coumarin ring and the presence of focused polar regions, with low bulk groups at the terminal ends of chalepin.[10] In fact a new series of coumarin derivatives was used to cross-validate this model.

Herein we describe the synthetic approach to obtain a series of 14 new 3-piperonylcoumarin derivatives, which were proposed as potential gGAPDH inhibitors, as well as new modeling studies that support a new binding mode for these coumarin derivatives.

In order to better understand the behavior of these compounds on the inhibition of *T. cruzi* gGADPH enzyme and to generate chemical data useful for the computer-aided molecular design, a structure–activity relationship (SAR) study was performed using docking procedures, partial components analysis (PCA) and the recently proposed electronic indices methodology (EIM).[11] Based on their inhibitory activities and molecular structures, evidences were found that support a hypothesis of different mechanisms of inhibition. Moreover, the proposed binding model enlightens the structure–activity relationships among the series and suggests possible new modifications that might improve binding toward gGAPDH.

2. Results and discussion

The gGAPDH inhibitory activities obtained for natural coumarins[8] stimulated us to propose the synthesis of some new coumarin derivatives (Fig. 2), in which a piperonyl group was linked to position 3 of the coumarin ring, by analogy to the previously identified active flavones

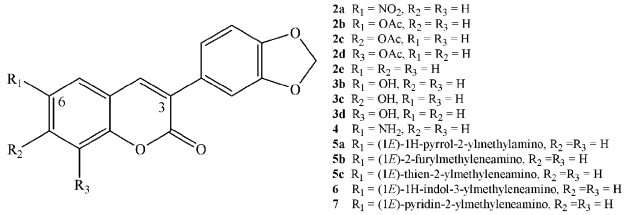

Figure 2. Target compounds designed as inhibitors of gGAPDH.

(Fig. 1).[7] These synthetic coumarins were proposed on the basis of some strategies for primary structure–activity relationship exploration, such as: (i) the appropriate substituent choice, as half of all existing drugs contain substituted aromatic rings; (ii) the easiness of the organic synthesis; and (iii) the elimination of the chiral centers.[12]

In order to estimate whether these new compounds would have reasonable inhibitory activity, preliminary docking studies using energy score evaluation function were undertaken. Compounds **5a**–**c** and **6** have shown score values similar to the one obtained for chalepin.[13] These initial results indicate that 3-piperonylcoumarin derivatives may be potential gGAPDH inhibitors. A simple synthetic strategy was designed to prepare these compounds and to test our initial hypothesis.

Compounds **2a**–**e** were synthesized by the Perkin–Oglialoro reaction of 3,4-(methylenedioxy)phenylacetic acid with salicylaldehyde derivatives, in Ac_2O and CH_3CO_2K (Scheme 1).[14,15] Electron-attracting groups on the salicylaldehyde ring increase the efficiency of the reaction, as observed for compound **2a**.[16] The deacetylation of compounds **2b**–**d** were carried out using HCl 2N in MeOH, affording compounds **3b**–**d** in good yields. Reduction of nitro-group in **2a** to afford **4** was efficiently achieved with $SnCl_2{\cdot}2H_2O$ in EtOH.[17] Compounds **5a**–**c**, **6**, and **7** were synthesized in good yields by the reaction of compound **4** with appropriate aromatic aldehydes, using molecular sieves as dehydration agents (Scheme 2).[18]

Structures of synthesized coumarins were established on the basis of ^1H and ^{13}C NMR spectra (see Experimental). The HMQC and HMBC experiments allowed us to completely attribute proton and carbon chemical shifts for compounds **5a**–**c**, **6**, and **7** (Table 1). NOE difference experiment for these coumarins showed NOEs between H-8′ and H-5/H-7, which confirm the stereochemistry *E* of imine bonds.

All coumarins synthesized were tested against gGAPDH, and the most significant results are shown in Table 2. Other coumarins were inactive in these concentrations. Coumarins **5a**, **5b**, and **6** showed the best inhibitory activities.

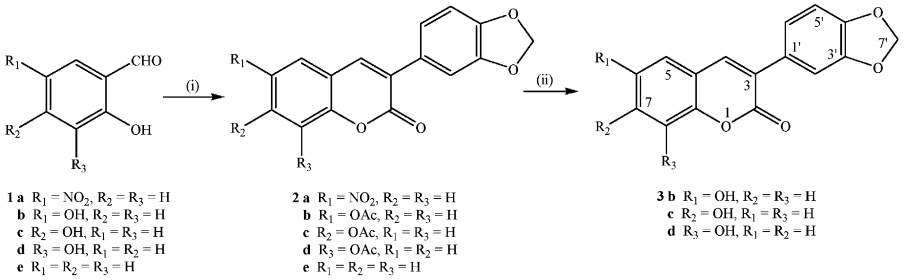

Scheme 1. Reagents: (i) 3,4-(methylenedioxy)phenylacetic acid, CH_3CO_2K, Ac_2O, reflux; (ii) HCl 2 N, MeOH.

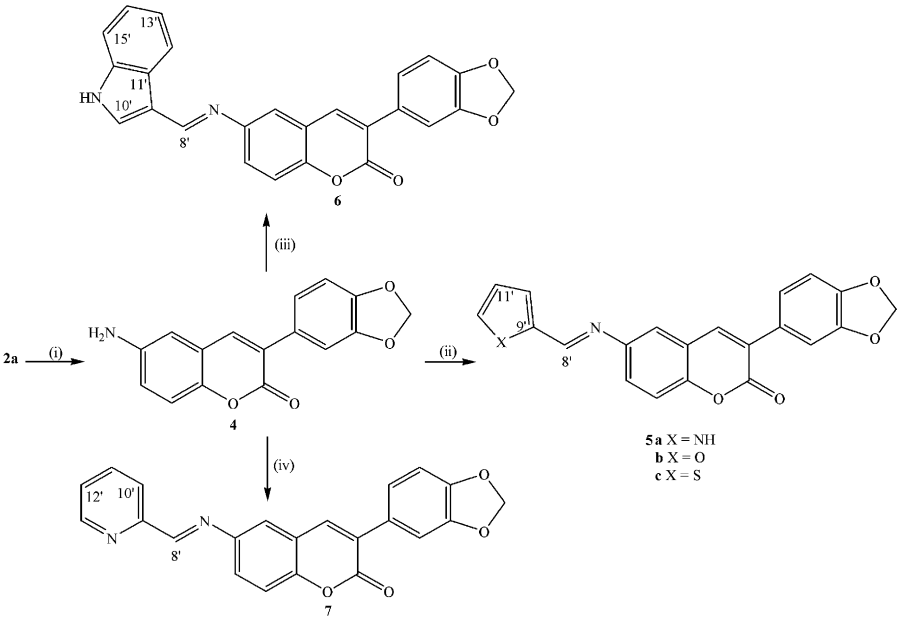

Scheme 2. Reagents: (i) $SnCl_2{\cdot}2H_2O$, EtOH, reflux; (ii) hetero-5-ring-2-carboxaldehydes, molecular sieves, benzene, reflux; (iii) indole-3-carboxaldehyde, molecular sieves, benzene, reflux; (iv) 2-pyridinecarboxaldehyde, molecular sieves, benzene, reflux.

Table 1. ^{1}H NMR data for coumarins **5a**–**c**, **6**, **7** (DMSO-d_6, 400 MHz)

H	5a	5b	5c	6	7
4	8.26 s	8.19 s	8.25 s	8.22 s	8.23 s
5	7.60 d (2.3)	7.63 d (2.5)	7.71 d (2.3)	7.59 d (2.3)	7.76 d (2.5)
7	7.51 dd (8.8; 2.3)	7.54 dd (8.8; 2.5)	7.61 dd (8.8; 2.3)	7.51 dd (8.8; 2.3)	7.66 dd (8.8; 2.5)
8	7.48 d (8.8)	7.46 d (8.8)	7.52 d (8.8)	7.45 d (8.8)	7.51 d (8.8)
2′	7.36 d (1.8)	7.31 d (1.8)	7.36 d (1.8)	7.32 d (1.8)	7.32 d (1.8)
5′	7.08 d (8.1)	7.03 d (8.1)	7.09 d (8.1)	7.03 d (8.1)	7.04 d (8.1)
6′	7.33 dd (8.1; 1.8)	7.27 dd (8.1; 1.8)	7.32 dd (8.1; 1.8)	7.28 dd (8.1; 1.8)	7.28 dd (8.1; 1.8)
7′	6.14 s	6.09 s	6.16 s	6.10 s	6.10 s
8′	8.43 s	8.52 s	8.93 d (1.0)	8.78 s	8.70 s
10′	6.81 m	7.21 dd (3.5; 0.8)	7.79 dd (3.5; 1.0)	8.06 s	8.20 dt (7.6; 1.0; 1.0)
11′	6.29 m	6.74 dd (3.3; 1.8)	7.31 dd (5.1; 3.5)	—	8.00 dt (7.6; 7.6; 1.8)
12′	7.12 m	7.98 d (1.8)	7.92 dt (5.1; 1.0; 1.0)	8.39 ddd (7.6; 1.5; 0.8)	7.57 ddd (7.6; 4.8; 1.0)
13′	—	—	—	7.20 dt (7.6; 7.6; 1.5)[a]	8.75 ddd (4.8; 1.8; 1.0)
14′	—	—	—	7.24 dt (7.6; 7.6; 1.8)[b]	—
15′	—	—	—	7.50 m	—
–NH	11.90 s	—	—	11.84 br s	—

[a,b] May be interchangeable.

It was not possible to estimate the IC_{50} values for all compounds by means of nonlinear fitting of untransformed data to the Michaelis–Menten equation. Most of the compounds precipitate due to low solubility in higher concentrations in reaction media. Therefore, bioactive compounds were considered the ones whose inhibitory concentrations were equal or lower than natural hit chalepin (IC_{50} 64 μM).[8]

Table 2. Inhibitory activities of gGAPDH (%)

Coumarin	Concentration (μM)				
	10	**25**	**35**	**45**	**60**
2b	nt	0	nt	29.6	30.0
3b	nt	0	nt	23.1	40.8
3c	nt	8.0	nt	22.2	29.1
5a	15.8	39.0	59.3	56.8	68.0
5b	16.0	22.0	37.0	46.0	nt
5c	18.5	19.4	24.7	28.7	35.0
6	17.1	32.3	37.3	48.3	60.8
7	4.0	4.3	15.0	14.5	12.9

nt—not tested.

2.1. SAR studies by electronic indices methodology (EIM) and CODESSA

The EIM is a new tool for SAR. It is a very efficient way to generate descriptors highly correlated to the biological activity at low computational cost, from quantum semi-empirical methods, using the local density of states (LDOS). LDOS is defined as the density of states (DOS) calculated over a specific region of the molecule using the coefficients from the linear combination of atomic orbitals (LCAO). This methodology has been successfully applied in other biological systems and has proven to improve the quality of SAR studies.[11] In this article, it was used for the first time together with the descriptors calculated with the CODESSA program.[19] This program generates several different types of descriptors automatically, from constitutional, topological and geometrical ones to electrostatical and quantum mechanical. It allows for the development of quantitative models of prediction for physical–chemical properties and biological activities.[20] In this paper, these two tools were used together to assay the inhibitory activity of coumarin analogs. The amount of information that can be obtained from quantum chemical calculations from single molecules combined with statistical exploratory techniques, such as cluster analysis, allows pinpointing the subtle causes of the observed variation in biological activity in some series of compounds. In addition, it can also help to understand the role of chemical groups when interacting with biological receptors.

One of the objectives of the EIM is to derive logical conditional relations based on the parameters Δ and η. These relations have proven to be useful to separate active from inactive compounds, one of the aims of SAR. The parameter η is a critical value derived from the LDOS calculated over a region of the molecule studied, which is important for the biological activity.

With the optimized geometries, eigenvalues and eigenvectors obtained, the density of states calculations is performed. The electronic density of states (DOS) is defined as the number of electronic states per energy unit. The related concept of local density of states (LDOS), that is the DOS calculated over a specific molecular region, is introduced in order to also describe the spatial distribution of the states over the system under consideration. For the LDOS calculations, the contribution of each atom to an electronic level is weighed by the square of the (real) molecular orbital coefficient, that is by the probability density corresponding to the level in that site. The summation is carried over the selected atomic orbitals (n_i to n_f), leading to the following expression (Eq. 1):[11]

$$\mathrm{LDOS}(E_i) = 2\sum_{m=n_i}^{n_f} |c_{mi}|^2 \tag{1}$$

The factor 2 comes from the Pauli's exclusion principle (maximum of 2 electrons per electronic level). This is a discrete modulation that allows a direct comparison of DOS and LDOS calculated from any linear combination of atomic orbital (LCAO) method. The EIM approach is based on two major descriptors, named η and Δ. The former, η, is related to the relative difference contribution between the most relevant molecular electronic levels over the identified molecular region linked to the biological activity (via LDOS) (Eq. 2):[11]

$$\eta = 2\sum_{m=n_i}^{n_f} (|c_{m\,\mathrm{level1}}|^2 - |c_{m\,\mathrm{level2}}|^2) \tag{2}$$

The second major EIM descriptor is Δ (Eq. 3). This descriptor is defined as the energy separation of the molecular levels from Eq. 2, leading to ΔH if the frontier levels are HOMO and HOMO − 1 and to ΔL if the frontier levels are LUMO and LUMO + 1. The same occurs for the ηL and ηH parameters.[11]

$$\Delta = E_{\mathrm{level1}} - E_{\mathrm{level2}} \tag{3}$$

After an extensive search over different regions, it was impossible to find values that could properly separate the active compounds from the inactive ones.

Most of the molecules presented the same behavior regarding the parameters used. The ΔL and ΔH values correspond to the energy gap between the HOMO and LUMO orbitals and the immediately molecular level.

The parameters ηL and ηH describe the different contribution of these orbitals to the LDOS over the carbons where chemical modifications took place to generate the compound series. One other reason for this choice was the chemical hypothesis of different influence of the aromaticity on the inhibitory activity of the hetero-ring substituted compounds of this series of coumarin derivatives. The different aromatic character of the hetero-ring substitutions of coumarins **5a**–**c**, **6**, **7** could influence the ηL and ηH critical values on the chosen atoms through resonance effect.

Almost all compounds show the same qualitative values, resulting in nothing that could lead to critical values to separate inactive from active ones. Despite this, one fact should be noticed: a group of active compounds with different values from most compounds. The coumarins **5a**–**5**, **6**, and **7** all containing hetero-aryl rings as substituents have lower molecular level energy gaps and negative values of ηL.

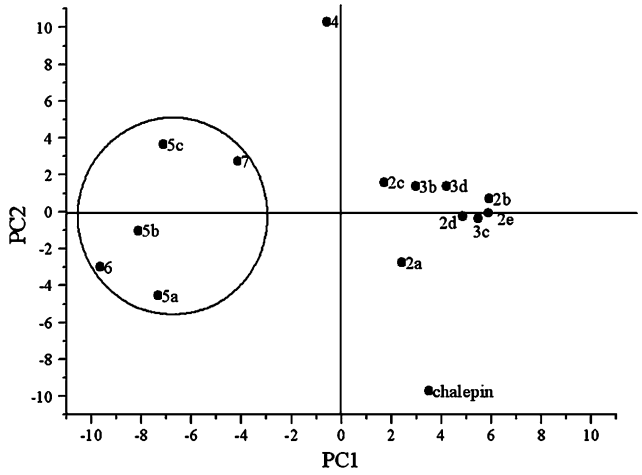

Figure 3. The score graph of the first two principal components (PC1 and PC2) for the inhibitory activities at 45 μM for the set of coumarin derivatives shown in Figure 2, using the four EIM (ηL, ηH, ΔH, and ΔL) descriptors.

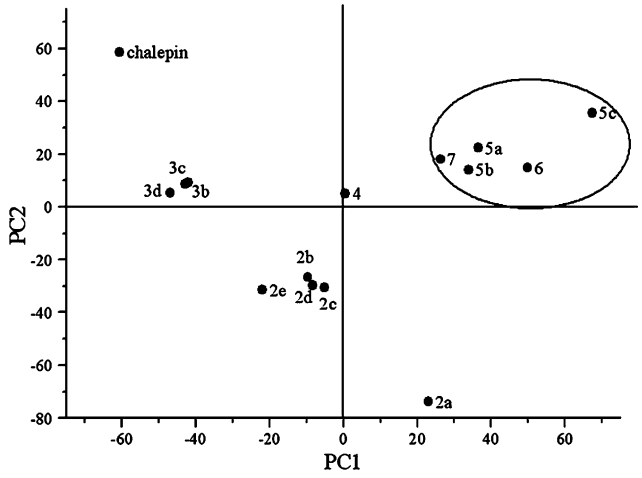

Figure 4. The score graph of the first two principal components (PC1 and PC2) for the inhibitory activities at 45 μM for the set of coumarin derivatives shown in Figure 2, using the 210 quantum-chemical descriptors from CODESSA and the EIM.

By combining the EIM descriptors with those generated with CODESSA and employing the cluster analysis, it was possible to verify that these compounds are chemically different regarding the inhibitory activity (Figs. 3 and 4). Over 200 different quantum-chemical descriptors were used (Fig. 4) and despite the possible high correlation between some of them, the inclusion of the EIM descriptors may ensure that a great amount of chemical information regarding reactivity and biological activity was used to cluster coumarins **5a**–**c**, **6**, and **7** when using the inhibitory activities at 45 μM as property to fit.

The same results were obtained with smaller sets of descriptors, where an initial screening pinpointed the better-correlated descriptors to the inhibitory activity. Chalepin in both cases appears separated from the other compounds. Although in both cases the PCA plot fails to separate the active compounds from the inactive ones, it was possible to cluster the molecules in different groups due the chemical substitutions regarding the biological activity. One possible explanation for these results is that chemically different coumarins would bind differently to the receptor, leading to different inhibition mechanisms. The low solubility of these coumarin derivatives in higher concentrations made it difficult to experimentally assay this hypothesis; alternatively a theorical approach was pursued as the best way to study the inhibition behavior of these compounds.

Docking results, presented in the next section, are in agreement with the ones found by the SAR assessment of the coumarin GADPH inhibitors.

2.2. Molecular modeling studies by docking

According to ligand molecular interaction fields (MIFs), Menezes et al.[10] proposed that bulkier groups at position 3 (analogous to 1,1-dimethyl-allyl in chalepin) would decrease inhibitory activity against gGAPDH. However, this study did not consider the available volume in *T. cruzi* gGAPDH active site for ligand binding. In fact, Figure 5 shows that heterocyclic derivatives (**5a**–**c**) would clash to protein residues, in case they interact with the same residues or crystallographic water molecules as chalepin.

This fact called our attention to another point, also raised by Menezes et al.;[10] whether or not coumarin derivatives would bind in the same way as chalepin to the receptor site. Aiming at investigating deeper this question, we undertook a different approach from that employed by Menezes et al.[10] Docking algorithms that use stochastic search methods, such as Monte Carlo or

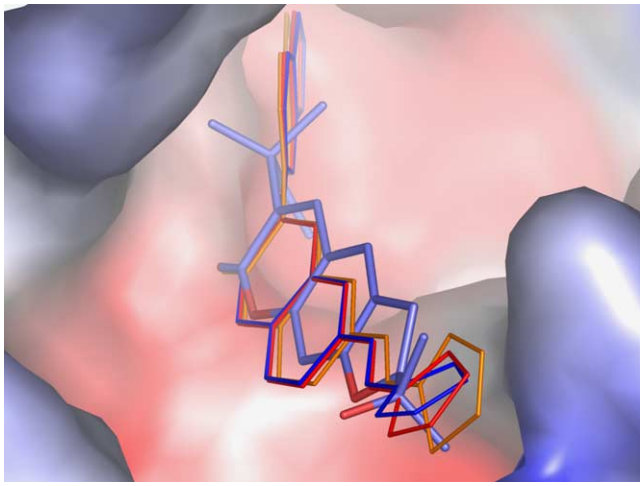

Figure 5. Structural superposition of compounds **5a**–**c** onto chalepin. Compounds were superposed using FLO, which considers chalepin crystallographic structure as the biologically active conformation and tries to fit compounds **5a**–**c** onto chalepin. Piperonyl moiety crashes to gGAPDH molecular surface (colored in the figure according to its electrostatic potential). Chalepin structure is presented in thick lines and compounds **5a** (blue), **5b** (red), and **5c** (orange) in thin lines.

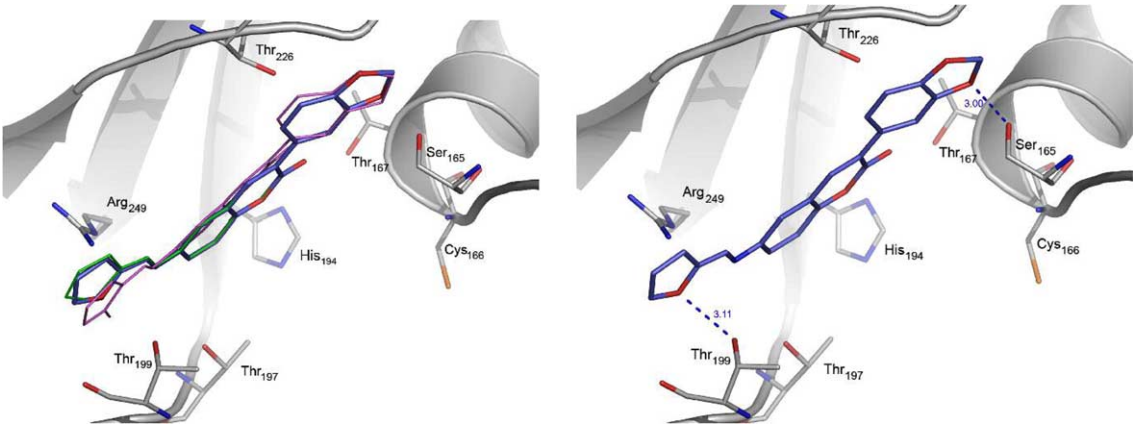

Figure 6. (Left) Compounds **5a–c** proposed interaction site. All compounds interact in the same region of gGAPDH active site with minor displacement in the heteroaromatic rings. (Right) Interaction profile of compound **5b** into gGAPDH active site. Compound **5b** hydrogen bonds to Ser^{165} and Thr^{199}. Compounds **5a** and **5c** have similar interaction profile to **5b**, but show different hydrogen bond strength to Thr^{199}. Protein atoms are presented in cartoon except for residues Ser^{165}, His^{194}, Thr^{199}, and Arg^{249} that interact to compounds **5a–c** or that are important for gGAPDH catalytic mechanism. Compound **5b** is represented in thick lines and compounds **5a** (purple) and **5c** (green) in thin lines.

Genetic algorithm, are known to produce poses (binding modes) that are close to the observed crystallographic positions.[21,22] For this reason, the docking software FLO[23] was used to establish reasonable binding modes for compounds **5a–c**, which additionally might clarify the different inhibitory profile of compound **5c**.

Docking studies were conducted as described in Experimental section, and according to modeling results, coumarin derivatives **5a**, **5b**, and **5c** show similar binding modes (Fig. 6). Modeled compounds are located in the region of the previously described inorganic phosphate binding site (residues Thr^{167}, Thr^{226}, Arg^{249})[24] and stretches across the substrate active site toward the substrate phosphate binding site (Thr^{197}, Thr^{199}, Arg^{249}).

This binding mode suggests that in compound **5b** 3′-methylenedioxi-oxygen hydrogen bonds to Ser^{165}, and its phenyl ring interacts to a hydrophobic pocket. Most of coumarin ring hangs in the solvent with no evident direct interaction with the protein (Fig. 7).

This binding mode might be a consequence of poor complementarity between the coumarin ring and gGAPDH active site. Indeed, chalepin–gGAPDH crystallographic structure supports this hypothesis since two interactions between chalepin and gGAPDH are mediated by water molecules in the crystallographic structure.[9] The hetero-5-ring moieties are located in the vicinity of Asp^{210} (not shown in figure), which call some attention since human GAPDH has a leucine residue in the equivalent position, and this difference is urged to be exploited for selective inhibition of *T. cruzi* gGAPDH.[25]

Small displacement is observed among docked inhibitors in the heterocyclic moiety at position 6 (Fig. 6). This behavior might be a consequence of a different requirement for hydrogen orientation for appropriate hydrogen bonding to Thr^{199}. In fact, the lack of a hydrogen bond between thiophene derivative (**5c**) and Thr^{199} affords a reasonable explanation for its decreased activity against *T. cruzi* gGAPDH, when compared with **5a** and **5b**.

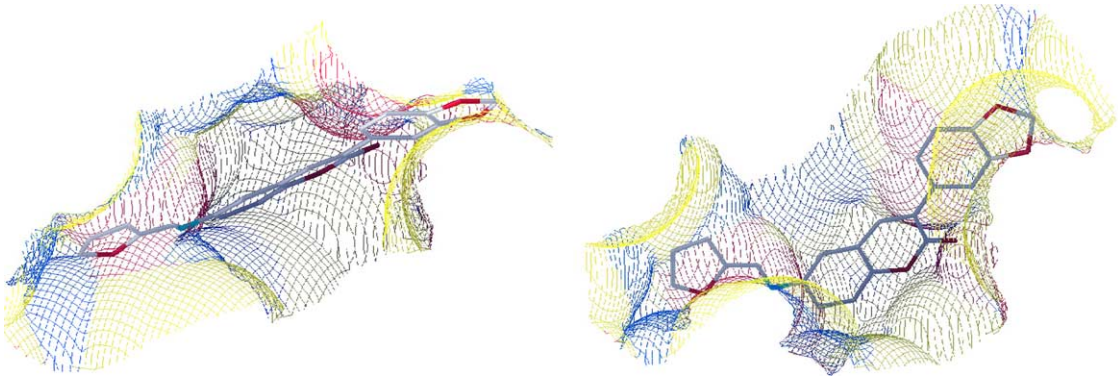

Figure 7. Proposed interaction profile of **5b** according to the gGAPDH solvent accessible surface (SAS). The figure shows two different views of compound **5b** complementarity to gGAPDH SAS. The two main interactions are: piperonyl moiety lies buried in a hydrophobic pocket (yellow), nevertheless its oxygen is oriented to hydrogen bond to Ser^{164} (not presented in the figure) and the furane ring, which lies close to a hydrogen donor region (red), where it hydrogen bonds to Thr^{199} (not presented in the figure). The coumarin ring hangs in the solvent away from gGAPDH SAS.

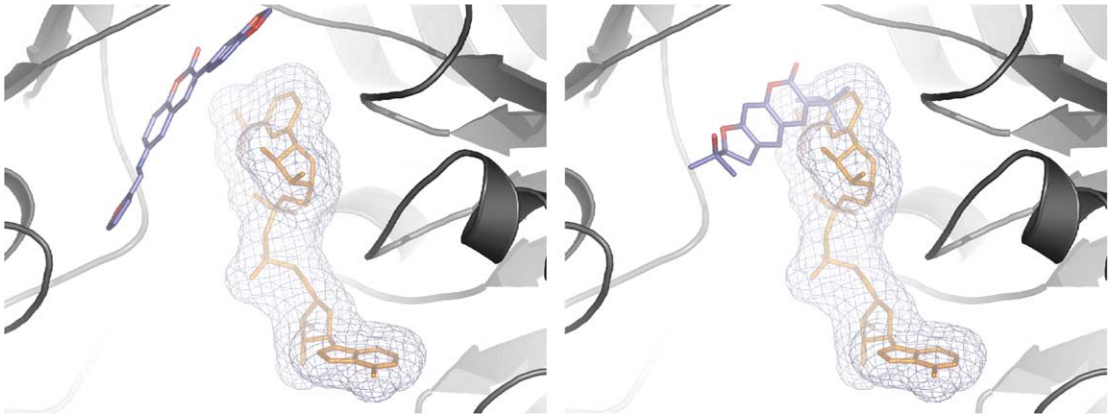

Figure 8. (Left) Proposed binding mode for **5b** in the gGAPDH active site suggests that no clash with NAD^+ molecule would occur. (Right) Binding mode of chalepin,[9] which would be the same for coumarins **2a–e** and **3d–d**. These coumarins would clash with the co-factor molecule in the active site.

In the case of compound **7**, not accounted for in modeling studies, the π-deficient character of the pyridine ring would not favor a possible charge-transfer complex interaction with Arg^{249}. On the other hand, this interaction would be stronger in active compounds **5a–c** and **6**, with π-excessive heterocyclic rings. Moreover, compound **7** would not be able to perform the hydrogen bonding with Thr^{199}, leading to a lower inhibitory activity.

Coumarins **2a–e** and **3b–d** showed weaker inhibitory activities than heterocyclic derivatives, reinforcing the role of heterocyclic rings in gGAPDH inhibition. Moreover, the docking experiments suggest that these two groups of coumarin derivatives should have different binding modes in the gGAPDH active site. While compounds **2a–e** and **3b–d** might interact as observed for chalepin,[9] in the substrate and co-factor regions, heterocyclic derivatives **5a–c**, **6**, and **7** would interact only in the substrate region (Fig. 8).

3. Conclusion

A tentative conclusion from the proposed binding model would be that, for this series of compounds, coumarin ring acts only as a spacer group that allows moieties at position 3 and 6 to interact with gGAPDH.

This hypothesis is supported by the fact that compounds that do not have the proper features to hydrogen bond to Thr^{199} prevent the inhibitor from being strongly attached to the binding site. In this case the lack of complementarity between the ligands and the gGAPDH binding site, associated with poor interaction profile (small number of hydrogen bonds, Van der Waals contacts, etc.) would not prevail over the desolvation penalty from binding, resulting at last in the absence of inhibitory activity.

The EIM methodology was able to describe these interaction features, indicating differences in the quantum-chemical profile of the coumarin derivatives presented here with an inexpensive computational effort.

Although the statistical exploratory technique employed was not able to qualitatively separate active compounds from inactive ones, and it was possible to achieve the same results as those from the docking approach, there are different binding modes between the synthetic coumarins and the GAPDH enzyme. This conclusion was achieved using only the physical–chemical properties of the ligands and the inhibitory activities in the statistical approach, and reinforced with much more detail through the docking analyses of the interactions between the receptor and ligands.

4. Experimental

General. Mp: Fisher-Johns 12144 melting-point apparatus. ^1H and ^{13}CNMR spectra: Bruker DRX500 spectrometer at 500 and 125 MHz, Bruker DRX400 spectrometer at 400 and 100 MHz or Bruker BPX300 spectrometer at 300 and 75 MHz, chemical shifts δ in ppm with $SiMe_4$ as an internal standard, coupling constants J in Hz. Elemental analyses were carried in Carlo Erba EA1110-CHNS-*O* and Fisons EA1108-CHNS-*O* instruments. Low resolution mass spectra were recorded on a VG Platform with electrospray ionization (ESI).

4.1. General synthetic procedure

4.1.1. 3-(1,3-Benzodioxol-5-yl)-6-nitro-2*H*-chromen-2-one (2a). A mixture of the 2-hydroxy-5-nitrobenzaldehyde (**1**, 1.39 g, 8.33 mmol), anhydrous CH_3CO_2K (1.42 g, 14.50 mmol), and 3,4-(methylenedioxy)phenylacetic acid (1.50 g, 8.33 mmol) in Ac_2O (5.68 mL) was refluxed (140 °C) with stirring for 49 h. The mixture was cooled, neutralized with $NaHCO_3$ 10%, and filtered. The yellow solid obtained (**2a**) was washed with H_2O, EtOAc and dried (2.59 g, 8.32 mmol, 91%). Mp: 274–275 °C.

^1H NMR (400 MHz, DMSO-d_6): 8.73 (d, J 2.5 Hz, H-5), 8.41 (dd, J 9.1, 2.5 Hz, H-7), 8.37 (s, H-4), 7.66 (d, J 9.1 Hz, H-8), 7.30 (d, J 1.8 Hz, H-2′), 7.29 (dd, J 8.1, 1.8 Hz, H-6′), 7.05 (d, J 8.1 Hz, H-5′), 6.10 (s, H-7′).

^{13}C NMR (100 MHz, DMSO-d_6): 159.2 (s), 156.7 (s), 148.4 (s), 147.6 (s), 143.9 (s), 138.7 (d), 128.5 (s), 128.1 (s), 126.3 (d), 124.5 (d), 123.1 (d), 120.3 (s), 117.7 (d), 109.1 (d), 108.6 (d), 101.8 (t).

Anal. Calcd for $C_{16}H_9NO_6$ (311): C, 61.74; H, 2.91; N, 4.50. Found: C, 61.75; H, 3.06; N, 4.58.

4.1.2. 3-(1,3-Benzodioxol-5-yl)-2-oxo-2*H*-chromen-6-yl-acetate (2b). A mixture of the 2,5-dihydroxy-benzaldehyde (**1b**, 231 mg, 1.67 mmol), anhydrous CH_3CO_2K (289 mg, 2.94 mmol), and 3,4-(methylenedioxy)phenylacetic acid (300 mg, 1.67 mmol) in Ac_2O (1.2 mL) was refluxed (140 °C) with stirring for 5 h. The mixture was cooled, neutralized with $NaHCO_3$ 10%, filtered, and extracted with EtOAc (2 × 20 mL). The organic layers were dried (anhydrous Na_2SO_4), filtered, and evaporated under reduced pressure. Compound **2b** was purified by recrystallization on EtOAc as a yellow solid (138 mg, 0.43 mmol, 30%). Mp: 173–174 °C.

^{1}H NMR (400 MHz, $CDCl_3$): 7.69 (s, H-4), 7.36 (d, *J* 8.8 Hz, H-8), 7.29 (d, *J* 2.8 Hz, H-5), 7.26 (dd, *J* 8.8, 2.8 Hz, H-7), 7.22 (d, *J* 1.8 Hz, H-2′), 7.18 (dd, *J* 8.1, 1.8 Hz, H-6′), 6.88 (d, *J* 8.1 Hz, H-5′), 6.02 (s, H-7′), 2.35 (s, OAc).

^{13}C NMR (100 MHz, $CDCl_3$): 169.4 (s), 160.4 (s), 150.8 (s), 148.5 (s), 147.8 (s), 146.7 (s), 138.2 (d), 128.7 (s), 128.3 (s), 124.7 (d), 122.7 (d), 120.1 (s), 119.9 (d), 117.5 (d), 109.1 (d), 108.4 (d), 101.4 (t), 21.1 (q).

MS *m*/*z* 325 $(M+1)^+$.

Anal. Calcd for $C_{18}H_{12}O_6$ (324): C, 66.67; H, 3.73. Found: C, 66.02; H, 3.81.

4.1.3. 3-(1,3-Benzodioxol-5-yl)-2-oxo-2*H*-chromen-7-yl-acetate (2c). This compound was prepared as described for **2a**, using 2,4-dihydroxy-benzaldehyde (**1c**, 231 mg, 1.67 mmol) in 25 h. After purification by recrystallization in EtOAc, compound **2c** was obtained as a yellow solid (146 mg, 0.45 mmol, 27%). Mp: 197–201 °C.

^{1}H NMR (400 MHz, $CDCl_3$): 7.66 (s, H-4), 7.45 (d, *J* 8.3 Hz, H-5), 7.15 (d, *J* 1.8, H-2′), 7.11 (dd, *J* 8.1, 1.8 Hz, H-6′), 7.07 (d, *J* 2.3 Hz, H-8), 6.99 (dd, *J* 8.3, 2.3 Hz, H-6), 6.81 (d, *J* 8.1 Hz, H-5′), 5.94 (s, H-7′), 2.28 (s, OAc).

^{13}C NMR (100 MHz, $CDCl_3$): 168.8 (s), 160.3 (s), 153.8 (s), 152.6 (s), 148.3 (s), 147.8 (s), 138.4 (d), 128.43 (s), 128.40 (d), 127.3 (s), 122.6 (d), 118.5 (d), 117.5 (s), 110.0 (d), 109.1 (d), 108.4 (d), 101.4 (t), 21.1 (q).

MS *m*/*z* 347 $(M+Na)^+$.

Anal. Calcd for $C_{18}H_{12}O_6$ (324): C, 66.67; H, 3.73. Found: C, 66.50; H, 3.79.

4.1.4. 3-(1,3-Benzodioxol-5-yl)-2-oxo-2*H*-chromen-8-yl-acetate (2d). This compound was prepared as described for **2a** and **2b**, using 2,3-dihydroxy-benzaldehyde (**1d**, 231 mg, 1.67 mmol) in 2 h. After purification by recrystallization in EtOAc, compound **2d** was obtained as a yellow solid (92 mg, 0.29 mmol, 17%). Mp: 193–195 °C.

^{1}H NMR (400 MHz, $CDCl_3$): 7.74 (s, H-4), 7.40 (m, H-6), 7.27 (m, H-5/H-7), 7.21 (d, *J* 2.0 Hz, H-2′), 7.17 (dd, *J* 8.1, 2.0 Hz, H-6′), 6.88 (d, *J* 8.1 Hz, H-5′), 6.02 (s, H-7′), 2.43 (s, OAc).

^{13}C NMR (125 MHz, $CDCl_3$): 168.6 (s), 159.4 (s), 148.5 (s), 147.8 (s), 145.1 (s), 138.5 (d), 137.6 (s), 128.6 (s), 128.4 (s), 125.2 (d), 124.7 (d), 124.2 (d), 122.6 (d), 121.1 (s), 109.1 (d), 108.4 (d), 101.4 (t), 20.7 (q).

MS *m*/*z* 325 (M+1); 347 $(M+Na)^+$.

Anal. Calcd for $C_{18}H_{12}O_6$ (324): C, 66.67; H, 3.73. Found: C, 67.22; H, 3.97.

4.1.5. 3-(1,3-Benzodioxol-5-yl)-2*H*-chromen-2-one (2e). A mixture of the 2-hydroxy-benzaldehyde **1e** (0.21 mL, 2.0 mmol), CH_3CO_2K (345 mg, 3.52 mmol), and 3,4-(methylenedioxy)phenylacetic acid (360 mg, 2.0 mmol) in Ac_2O (1.4 mL) was refluxed (140 °C) with stirring for 5 h. The mixture was cooled, neutralized with $NaHCO_3$ 10%, filtered, and extracted with EtOAc (2 × 20 mL). The organic layers were dried (Na_2SO_4), filtered, and evaporated under reduced pressure. The product was purified by recrystallization in EtOH, yielding compound **2e** as a yellow solid (131 mg, 0.49 mmol, 25%). Mp: 169–171 °C.

^{1}H NMR (400 MHz, $CDCl_3$): 7.76 (s, H-4), 7.53 (d, *J* 7.6 Hz, H-8), 7.52 (dt, *J* 7.6, 7.6, 1.0 Hz, H-7), 7.36 (br d, *J* 7.6 Hz, H-5), 7.29 (dt, *J* 7.6, 7.6, 1.0 Hz, H-6), 7.24 (d, *J* 1.8 Hz, H-2′), 7.19 (dd, *J* 8.1, 1.8 Hz, H-6′), 6.88 (d, *J* 8.1 Hz, H-5′), 6.00 (s, H-7′).

^{13}C NMR (100 MHz, $CDCl_3$): 160.7 (s), 153.3 (s), 148.3 (s), 147.7 (s), 139.0 (d), 131.3 (d), 128.6 (s), 127.9 (s), 127.8 (d), 124.5 (d), 122.5 (d), 119.7 (s), 116.4 (d), 109.1 (d), 108.4 (d), 101.4 (t).

MS *m*/*z* 267 $(M+H)^+$.

Anal. Calcd for $C_{16}H_{10}O_4$ (266): C, 72.18; H, 3.79. Found: C, 72.66; H, 3.94.

4.1.6. 3-(1,3-Benzodioxol-5-yl)-6-hydroxy-2*H*-chromen-2-one (3b). A mixture of coumarin **2b** (80 mg, 0.25 mmol) and aqueous solution of HCl 2 N (10 mL) in MeOH (3 mL) was refluxed for 2 h (100 °C). Product **3b** was obtained as a solid, which was filtered from the reaction mixture and washed in cooled water. After drying it was obtained 36.4 mg (0.13 mmol) of coumarin **3b** (53%). Mp: 234–238 °C.

^{1}H NMR (400 MHz, CD_3OD): 7.82 (s, H-4), 7.14–7.10 (m, H-8), 7.13 (dd, *J* 1.8, 0.5 Hz, H-2′), 7.12 (dd, *J* 8.1, 1.8 Hz, H-6′), 6.96–6.92 (m, H-5 and H-7), 6.79 (dd, *J* 8.1, 0.5 Hz, H-5′), 5.90 (s, H-7′).

^{13}C NMR (125 MHz, CD_3OD): 162.9 (s), 155.5 (s), 149.5 (s), 149.0 (s), 148.2 (s), 141.1 (d), 130.2 (s), 128.6

(s), 123.7 (d), 121.7 (s), 120.8 (d), 117.9 (d), 113.5 (d), 110.1 (d), 109.1 (d), 102.7 (t).

MS *m/z* 283 $(M+H)^+$.

Anal. Calcd for $C_{16}H_{10}O_5$ (282): C, 68.09; H, 3.57. Found: C, 68.14; H, 3.99.

4.1.7. 3-(1,3-Benzodioxol-5-yl)-7-hydroxy-2*H*-chromen-2-one (3c). A mixture of coumarin **2c** (100 mg, 0.31 mmol) and aqueous solution of HCl 2 N (10 mL) in MeOH (3 mL) was refluxed for 4 h (100 °C). Product **3c** was obtained as a solid, which was filtered from the reaction mixture and washed in cooled water. After drying it was obtained 78 mg (0.27 mmol) of coumarin **3c** (90%). Mp: 240–243 °C.

^{1}H NMR (400 MHz, CD_3OD): 7.95 (s, H-4), 7.53 (d, *J* 8.6 Hz, H-5), 7.23 (d, *J* 1.8 Hz, H-2′), 7.20 (dd, *J* 8.1, 1.8 Hz, H-6′), 6.89 (d, *J* 8.1 Hz, H-5′), 6.82 (dd, *J* 8.6, 2.3 Hz, H-6), 6.75 (d, *J* 2.3 Hz, H-8), 6.00 (s, H-7′).

^{13}C NMR (100 MHz, CD_3OD): 162.9 (s), 156.5 (s), 150.2 (s), 149.5 (s), 149.1 (s), 141.8 (d), 130.8 (d), 130.6 (s), 124.2 (s), 123.4 (d), 114.8 (d), 113.9 (s), 110.0 (d), 109.1 (d), 103.0 (d), 102.7 (t).

MS *m/z* 305 $(M+Na)^+$.

Anal. Calcd for $C_{16}H_{10}O_5$ (282): C, 68.09; H, 3.57. Found: C, 68.06; H, 3.90.

4.1.8. 3-(1,3-Benzodioxol-5-yl)-8-hydroxy-2*H*-chromen-2-one (3d). A mixture of coumarin **2d** (60 mg, 0.19 mmol) and aqueous solution of HCl 2 N (10 mL) in MeOH (3 mL) was refluxed for 2 h (100 °C). Product **3d** was obtained as a solid, which was filtered from the reaction mixture and washed in cooled water. After drying, it was obtained 46.5 mg (0.17 mmol) of coumarin **3d** (89%). Mp: 242–245 °C.

^{1}H NMR (400 MHz, CD_3OD): 7.89 (s, H-4), 7.16 (dd, *J* 1.8, 0.5 Hz, H-2′), 7.14 (dd, *J* 8.1, 2.0 Hz, H-6′), 7.07 (dd, *J* 7.8, 7.3 Hz, H-6), 7.04 (dd, *J* 7.8, 2.3 Hz, H-5), 6.97 (dd, *J* 7.3, 2.3 Hz, H-7), 6.80 (dd, *J* 8.1, 0.5 Hz, H-5′), 5.90 (s, H-7′).

^{13}C NMR (125 MHz, CD_3OD): 161.3 (s), 153.2 (s), 148.5 (s), 148.1 (s), 144.7 (s), 140.6 (d), 129.2 (s), 127.4 (s), 124.9 (d), 122.7 (d), 121.0 (s), 118.9 (d), 118.1 (d), 109.1 (d), 108.1 (d), 101.4 (t).

MS *m/z* 283 $(M+H)^+$.

Anal. Calcd for $C_{16}H_{10}O_5$ (282): C, 68.09; H, 3.57. Found: C, 68.01; H, 3.70.

4.1.9. 6-Amino-3-(1,3-benzodioxol-5-yl)-2*H*-chromen-2-one (4). A mixture of coumarin **2a** (3.20 g, 10.3 mmol) and $SnCl_2{\cdot}2H_2O$ (11.59 g, 51.5 mmol) in EtOH (20 mL) was refluxed (80 °C) with stirring for 9 h, under N_2 atmosphere. The mixture was cooled, neutralized with $NaHCO_3$ 10%, filtered, and extracted with EtOAc (8×20 mL). The organic layers were dried (Na_2SO_4), filtered, and evaporated under reduced pressure, affording coumarin **4** (yellow solid) as a pure compound (1.79 g, 6.37 mmol, 62%). Mp: 202–204 °C.

^{1}H NMR (400 MHz, DMSO-d_6): 8.10 (s, H-4), 7.35 (d, *J* 1.8 Hz, H-2′), 7.30 (dd, *J* 8.1, 1.8 Hz, H-6′), 7.18 (d, *J* 8.8 Hz, H-8), 7.05 (d, *J* 8.1, H-5′), 6.91 (dd, *J* 8.8, 2.8 Hz, H-7), 6.85 (d, *J* 2.8 Hz, H-5), 6.10 (s, H-7′), 5.32 (br s, NH_2).

^{13}C NMR (100 MHz, DMSO-d_6): 160.5 (s), 147.7 (s), 147.4 (s), 146.0 (s), 144.9 (s), 140.3 (d), 129.2 (s), 126.1 (s), 122.9 (d), 120.2 (s), 118.9 (d), 116.4 (d), 110.5 (d), 109.3 (d), 108.4 (d), 101.6 (t).

MS *m/z* 282 $(M+H)^+$.

Anal. Calcd for $C_{16}H_{11}NO_4$ (281): C, 68.32; H, 3.94; N, 4.98. Found: C, 67.78; H, 4.24; N, 5.46.

4.2. General procedure for the preparation of heteroaromatic coumarins (5a–c, 6, 7)

The solutions containing 3-(3,4-methylenedioxyphenyl)-6-aminocoumarin (**4**) (0.25 mmol), appropriated heteroaromatic aldehydes (0.375 mmol), and 790 mg of molecular sieves in 6 mL of anhydrous benzene were refluxed under N_2 at 80 °C for 29 h. The mixtures obtained were filtered through Celite, which was washed with hot $CHCl_3$. Resulting solutions were concentrated to give crude products, which were recrystallized in the solvents indicated bellow to afford the heteroaromatic coumarins.

4.2.1. 3-(1,3-Benzodioxol-5-yl)-6-{[(1*E*)-1*H*-pyrrol-2-ylmethylene]amino}-2*H*-chromen-2-one (5a). Recrystallized in EtOH (62% yield), mp 212–214 °C; ^{1}H NMR (400 MHz): Table 1.

^{13}C NMR (100 MHz, DMSO-d_6): 160.0 (C-2), 151.2 (C-8′), 150.5 (C-8a), 148.7 (C-6), 147.8 (C-4′), 147.4 (C-3′), 139.8 (C-4), 130.6 (C-9′), 128.7 (C-1′), 126.8 (C-3), 124.6 (C-7), 124.4 (C-12′), 122.8 (C-6′), 120.2 (C-4a), 119.6 (C-5), 117.1 (C-10′), 116.8 (C-8), 110.1 (C-11′), 109.0 (C-2′), 108.3 (C-5′), 101.5 (C-7′).

MS *m/z* 359 $(M+H)^+$.

Anal. Calcd for $C_{21}H_{14}N_2O_4$ (358): C, 70.39; H, 3.94; N, 7.82. Found: C, 69.82; H, 4.03; N, 7.58.

4.2.2. 3-(1,3-Benzodioxol-5-yl)-6-{[(1*E*)-2-furylmethylene]amino}-2*H*-chromen-2-one (5b). Recrystallized in EtOH (76% yield), mp 199–202 °C; ^{1}H NMR (400 MHz): Table 1.

^{13}C NMR (100 MHz, DMSO-d_6): 159.7 (C-2), 151.7 (C-9′), 151.0 (C-8a), 148.8 (C-8′), 147.6 (C-3′), 147.3 (C-4′), 147.1 (C-6), 146.7 (C-12′), 139.4 (C-4), 128.4 (C-1′), 126.8 (C-3), 124.3 (C-7), 122.6 (C-6′), 120.1 (C-5), 120.0 (C-4a), 117.5 (C-10′), 116.7 (C-8), 112.6 (C-11′), 108.8 (C-2′), 108.1 (C-5′), 101.3 (C-7′).

MS *m/z* 360 $(M+H)^+$.

Anal. Calcd for $C_{21}H_{13}NO_5$ (359): C, 70.19; H, 3.65; N, 3.90. Found: C, 69.70; H, 3.66; N, 4.29.

4.2.3. 3-(1,3-Benzodioxol-5-yl)-6-{[(1*E*)-thien-2-ylmethylene]amino}-2*H*-chromen-2-one (5c). Recrystallized in EtOH (77% yield), mp 214–216 °C; ^{1}H NMR (400 MHz): Table 1.

^{13}C NMR (100 MHz, DMSO-d_6): 160.0 (C-2), 154.8 (C-8′), 151.3 (C-8a), 148.0 (C-4′), 147.4 (C-3′), 147.3 (C-6), 142.5 (C-9′), 139.7 (C-4), 134.3 (C-10′), 131.8 (C-12′), 128.7 (C-1′), 127.1 (C-11′), 124.6 (C-7), 122.9 (C-6′), 120.7 (C-5), 120.3 (C-4a), 117.0 (C-8), 109.1 (C-2′), 108.4 (C-5′), 101.6 (C-7′).

EIMS *m/z* 376 $(M+H)^+$.

Anal. Calcd for $C_{21}H_{13}NO_4S$ (375): C, 67.19; H, 3.49; N, 3.73; S, 8.54. Found: C, 67.15; H, 3.54; N, 3.36; S, 8.59.

4.2.4. 3-(1,3-Benzodioxol-5-yl)-6-{[(1*E*)-1*H*-indol-3-ylmethylene]amino}-2*H*-chromen-2-one (6). Recrystallized in EtOAc (37% yield), mp 248–250 °C; ^{1}H NMR (400 MHz): Table 1.

^{13}C NMR (100 MHz, DMSO-d_6): 160.2 (C-2), 156.4 (C-8′), 150.5 (C-8a), 150.0 (C-6), 147.5 (C-4′), 140.1 (C-4), 137.6 (C-16′), 134.3 (C-10′), 128.9 (C-1′), 126.9 (C-3), 125.1 (C-11′), 124.9 (C-7), 123.3 (C-6′), 123.0 (C-12′), 122.1 (C-13′), 121.4 (C-14′), 119.7 (C-5), 118.4 (C-4a), 116.8 (C-8), 115.3 (C-9′), 112.4 (C-15′), 109.2 (C-2′), 108.5 (C-5′), 101.7 (C-7′).

MS *m/z* 409 $(M+H)^+$.

Anal. Calcd for $C_{25}H_{16}N_2O_4$ (408): C, 73.52; H, 3.95; N, 6.86. Found: C, 72.95; H, 4.23; N, 6.83.

4.2.5. 3-(1,3-Benzodioxol-5-yl)-6-{[(1*E*)-pyridin-2-ylmethylene]amino}-2*H*-chromen-2-one (7). Recrystallized in EtOH (34% yield), mp 256–259 °C; ^{1}H NMR (400 MHz): Table 1.

^{13}C NMR (100 MHz, DMSO-d_6): 159.9 (C-2), 156.1 (C-8′), 152.6 (C-6), 150.3 (C-8a), 147.4 (C-4′), 147.1 (C-3′), 145.6 (C-9′), 144.6 (C-13′), 140.0 (C-4), 137.8 (C-11′), 128.9 (C-1′), 128.5 (C-12′), 126.9 (C-3), 126.1 (C-7), 122.6 (C-6′), 121.8 (C-10′), 119.7 (C-5), 118.6 (C-4a), 116.1 (C-8), 108.9 (C-2′), 108.1 (C-5′), 101.3 (C-7′).

MS *m/z* 409 $(M+K)^+$.

Anal. Calcd for $C_{22}H_{14}N_2O_4$ (370): C, 71.35; H, 3.81; N, 7.56. Found: C, 71.68; H, 3.87; N, 7.60.

4.3. Biochemical assays

The gGAPDH used in the assays is a recombinant enzyme obtained in an *Escherichia coli* expression system. The preparation and purification of the gGAPDH followed the procedure previously described.[25] The assays were performed as described,[8] using 1.5 μg protein in each experiment. All coumarins synthesized were tested in four or five concentrations: **2a**: 10, 20, 25, 30, 40 μM; **2b–e**, **3b–d**: 25, 45, 60, 80, 100 μM; **4**: 10, 25, 45, 60, 80 μM; **5a**, **5c**, **6**, **7**: 10, 25, 35, 45, 60 μM; **5b**: 10, 25, 35, 45 μM. Coumarins **2a**, **4**, **5a–c**, **6**, **7** precipitate in higher concentrations than those tested. All the measurements were run in triplicate. A negative control with 10% DMSO was used.

4.4. General docking strategy

Modeling studies can be divided in the following sequential steps: Compounds **5a–c** and **6** were built and had their potentials assigned in FLO,[23] manual potential correction was applied when necessary. *T. cruzi* gGAPDH coordinates from chalepin–gGAPDH complex (PDB code 1K3T) was selected for docking studies and its polar hydrogen atoms were added and potentials assigned automatically. Searches were carried out using a modified Monte Carlo energy minimization method, which according to Bohacek & Martin produce near native conformations for the inhibitor in the active site.[23] Visual-analysis of the 20 best solutions was performed and the best binding modes were selected for further energy minimization inside the active site of gGAPDH. This new protocol employs a superposition force field that automatically assigns short-range attractive forces to similar atoms in different molecules and therefore improves inhibitor–receptor complementarity. Compound **5b** best solution was selected as a framework upon which all other inhibitors were built and energy minimized into gGAPDH's active site. This procedure, which afforded a reasonable binding mode that despite low complementarity, explains qualitatively the structure–activity relationship among coumarins **5a–c**. Just for a matter of cross-validation, all ligands were subject to a full Monte Carlo search with subsequent energy minimization. The final docking scores and binding mode are not significantly different from the previous results.

4.5. SAR studies and EIM methodology

In order to compare the descriptors generated for different molecules, all molecular geometries were optimized until the gradient of the hypersurface of energy reaches 0.01 kJ/mol with the semi-empirical PM3[26] method within MOPAC 6.0 program.[27] An exhaustive conformational search was performed and the geometries found were compared with the ones obtained from molecular mechanics methods. The EIM parameters were calculated with the CHEM2PAC program.[28]

The parameters of the PCA calculations, used to perform the cluster analysis, discussed elsewhere, were the default options on CODESSA.

Acknowledgements

The authors are grateful to FAPESP (processes 98/14107-0, 01/05617-9, 00/01688-6) and CNPq (process 142008/

01-0) for the financial support and research fellowships. Thanks to Professor Douglas Galvão from GSOMN, Instituto de Física, UNICAMP, for encouraging us to apply the EIM, and to Instituto de Quimica, UNESP, Araraquara, for the obtainment of Mass Spectra.

References and notes

1. Urbina, J. A.; DoCampo, R. *Trends Parasitol.* **2003**, *11*, 495.
2. Coura, J. R.; Castro, S. L. *Mem. Inst. Oswaldo Cruz* **2002**, *97*, 3.
3. Lambeir, A. M.; Loiseau, A. M.; Kuntz, D. A.; Vellieux, F. M.; Michels, P. A. M.; Opperdoes, F. R. *Eur. J. Biochem.* **1991**, *198*, 429.
4. Bakker, B. M.; Michels, P. A. M.; Opperdoes, F. R.; Westerhoff, H. V. *J. Biol. Chem.* **1999**, *274*, 14551.
5. Kennedy, K. J.; Bressi, J. C.; Gelb, M. H. *Bioorg. Med. Chem. Lett.* **2001**, *11*, 95.
6. Schuster, R.; Holzhütter, H. G. *Eur. J. Biochem.* **1995**, *229*, 403.
7. Tomazela, D. M.; Pupo, M. T.; Passador, E. A. P.; Silva, M. F. G. F.; Vieira, P. C.; Fernandes, J. B.; Rodrigues-Fo, E.; Oliva, G.; Pirani, J. R. *Phytochemistry* **2000**, *55*, 643.
8. Vieira, P. C.; Mafezoli, J.; Pupo, M. T.; Fernandes, J. B.; Silva, M. F. G. F.; Albuquerque, S.; Oliva, G.; Pavão, F. *Pure Appl. Chem.* **2001**, *73*, 617.
9. Pavão, F.; Castilho, M. S.; Pupo, M. T.; Dias, R. L. A.; Correa, A. G.; Fernandes, J. B.; Silva, M. F. G. F.; Mafezoli, J.; Vieira, P. C.; Oliva, G. *FEBS Lett.* **2002**, *520*, 13.
10. Menezes, I. R. A.; Lopes, J. C. D.; Montanari, C. A.; Oliva, G.; Pavão, F.; Castilho, M. S.; Vieira, P. C.; Pupo, M. T. *J. Comp. Aid. Mol. Des.* **2003**, *17*, 277.
11. Braga, R. S.; Vendrame, R.; Galvão, D. S. *J. Chem. Inf. Sci.* **2000**, *40*, 1377.
12. Wermuth, C. G. In *The Practice of Medicinal Chemistry*; Wermuth, C. G., Ed.; Academic: Cambridge, 1996; pp 295–306.
13. Marchi, A. A.; Jacoveto, D. C. M.; Archanjo, F. C.; Pupo, M. T.; Del Ponte, G.; Castilho, M. S.; Oliva, G. 1st Brazilian Symposium on Medicinal Chemistry 2001, Caxambú-MG, Brazil, PDD-2 (http://agora.grude.ufmg.br/brazmedchem).
14. Donnelly, D. M. X.; Kavanagh, P. J. *Phytochemistry* **1974**, *13*, 2587.
15. Murray, R. D. H.; Méndez, J.; Brown, S. A. *The Natural Coumarins*; John Wiley & Sons: Chichester, 1982; pp 131–137.
16. Norman, R. O. C.; Coxon, J. M. *Principles of Organic Synthesis*; Blackie Academic & Professional: Oxford, 1993; pp 218–219.
17. Bellamy, F. D.; Ou, K. *Tetrahedron Lett.* **1984**, *25*, 839.
18. Corey, E. J.; Shibata, S.; Bakshi, R. K. *J. Org. Chem.* **1988**, *53*, 2861.
19. Comprehensive Descriptors for Structural and Statistical Analysis (CODESSA), Semichem, Inc., 1995; p 199.
20. Menziani, M. C.; Benedetti, P. G.; Karelson, M. *Bioorg. Med. Chem.* **1998**, *6*, 535.
21. Morris, G. M.; Goodsell, D. S.; Halliday, R. S.; Huey, R.; Hart, W. E.; Belew, R. K.; Olson, A. J. *J. Comp. Chem.* **1998**, *19*, 1639.
22. Diller, D. J.; Verlinde, C. L. M. J. *J. Comp. Chem.* **1999**, *20*, 1740.
23. McMartin, C.; Bohacek, R. S. *J. Comp. Aid. Mol. Des.* **1997**, *11*, 333.
24. Castilho, M. S.; Ladame, S.; Pavão, F.; Willson, M.; Perie, J.; Oliva, G. *Biochemistry* **2003**, *42*, 7143.
25. Souza, D. H. F.; Garrat, R. C.; Araújo, A. P. U.; Guimarães, B. G.; Jesus, W. D. P.; Michels, P. A. M.; Hannaert, V.; Oliva, G. *FEBS Lett.* **1998**, *424*, 131.
26. Stewart, J. J. P. *J. Comput. Chem.* **1989**, *10*, 221.
27. MOPAC Program, version 6.0; Quantum Chemistry Exchange No. 455.
28. www.ifi.unicamp.br/gsnonm/chem2pac.